Phase stability in nanoscale material systems: extension from bulk phase diagrams

Saurabh Bajaj[a,*], Michael G. Haverty[b], Raymundo Arróyave[c,d], William A. Goddard III FRSC[a], Sadasivan Shankar[e]

[a] *Department of Applied Physics and Materials Science, California Institute of Technology, Pasadena, CA 91125, USA*
[b] *Process Technology Modeling, Design and Technology Solutions, Technology and Manufacturing Group, Intel Corporation, Santa Clara, CA 95052, USA*
[c] *Department of Materials Science and Engineering, Texas A&M University, College Station, TX 77843, USA*
[d] *Department of Mechanical Engineering, Texas A&M University, College Station, TX 77843, USA*
[e] *School of Engineering and Applied Sciences, Harvard University, Cambridge, MA 02138, USA*

S1. Computational methods

S1.1. The CALPHAD method

The method of CALculation of PHAse Diagrams (or CALPHAD for short) has been widely utilized to calculate bulk phase diagrams and thermodynamic properties of multi-component systems [S1]. It involves the use of Gibbs free energy models developed for various types of phases, such as random solutions (gases, liquids, and solids), sublattice phases, ionic phases, etc. Variables used in these models are calculated by fitting either to experimental data or *ab initio* calculations.

The CALPHAD method [S1] is well established for calculating bulk phase diagrams, and is a good starting point for calculating phase equilibria in nanoscale systems. In this work, since we have considered surface effects on binary solution phases, thermodynamic models for only these types of phases will be described. The Gibbs free energy of a bulk random solution phase ϕ is given by,

$$G_m^{\phi,bulk} = G_{ref} + \Delta G_{mix}^{ideal} + \Delta G_{mix}^{xs}, \tag{S1}$$

*Corresponding address: Department of Applied Physics and Materials Science, California Institute of Technology, Pasadena, CA 91125, USA, Tel.: +1 626-395-3982
Email address: sbajaj@caltech.edu (Saurabh Bajaj)

where, G_{ref} is the sum of standard Gibbs energies of each component, ΔG_{mix}^{ideal} is the ideal mixing configurational entropy contribution to the Gibbs free energy of the solution phases, and ΔG_{mix}^{xs}, called the excess energy of mixing, takes into account all the non-ideal temperature dependent effects such as interaction between components, non-ideal configurational entropy, vibrational and electronic entropy, etc. Expanding each term, Eqn. (S1) becomes,

$$\begin{aligned} G_m^{\phi,bulk} = & \sum_{i=A,B} x_i \, {}^oG_i^{bulk} \; + \; RT \sum_{i=A,B} x_i log_e x_i \; + \; \Delta G_{mix}^{xs} \\ = & \; x_A \, {}^oG_A^{bulk} \; + \; x_B \, {}^oG_B^{bulk} \; + RT(x_A log_e x_A \; + \; x_B log_e x_B) \; + \; \Delta G_{mix}^{xs}, \end{aligned} \tag{S2}$$

where, x_A and x_B are mole fractions of components A and B of the phase, respectively, and ${}^oG_A^{\phi,bulk}$ and ${}^oG_B^{\phi,bulk}$ are the standard Gibbs energies of the phase containing only the pure component A and B, respectively. These are obtained from the Scientific Group Thermodata Europe (SGTE) database [S2]. R is the gas constant, and T is the temperature. The excess Gibbs free energy of mixing ΔG_{mix}^{xs} is expanded according to the Redlich-Kister formalism [S3] as,

$$\Delta G_{mix}^{xs} \; = \; x_A x_B \sum_v L_v^{\phi} (x_A \; - \; x_B)^v, \tag{S3}$$

where, v is the order of expansion ($v \; = \; 0$ for regular solution phases and $v \; = \; 1$ or above for non-regular solution phases), and L_v^{ϕ} is called the non-ideal interaction parameter. As the excess Gibbs free energy of mixing must include temperature dependency of other sources of entropy (non-ideal configurational, vibrational, and electronic) apart from ideal configurational entropy, these parameters are further expanded as,

$$L_v^{\phi} \; = \; A_v^{\phi} \; + \; B_v^{\phi}.T, \tag{S4}$$

where, A_v^{ϕ} and B_v^{ϕ} are user-defined parameters that are calculated and optimized in the CALPHAD method with available experimental data on positions of equilibrium lines in the phase diagram, phase thermodynamic properties such as enthalpy and entropy of mixing, etc., and/or similar data calculated from *ab initio* calculations, which is particularly useful in cases where no experimental data is available.

References

[S1] N. Saunders, A.P. Miodownik, Pergamon Mater. Ser. (1998).

[S2] A.T. Dinsdale, CALPHAD 15 (1991) 317-425.

[S3] O. Redlich, A.T. Kister, Ind. Eng. Chem. 40 (1948) 345-348.

[S4] J. Lee, M. Nakamoto, T. Tanaka, J. Mater. Sci. 40 (2005) 21672171.

[S5] L.E. Murr, Interfacial Phenomena in Metals and Alloys, Addison-Wesley Publishing Company, London, 1975, p. 124.

[S6] F. Millot, V. Sarou-Kanian, J.C. Rifflet, B. Vinet, Mat. Sci. Eng. A 495(2008) 813.

[S7] R.J. Jaccodine, J. Electrochem. Soc. 110 (1963) 524-527.

[S8] T. Iida, R.I.L. Guthrie, The Physical Properties of Liquid Metals, Oxford Science Publications, (1993).

[S9] I. Sa, B.-M. Lee, C.-J. Kim, M.-H. Jo, B.-J. Lee, CALPHAD 32 (2008) 669-674.

[S10] K.C. Mills: Recommended values of thermophysical properties for selected commercial alloys, Woodhead Publishing Ltd., Cambridge, UK, 2002.

[S11] J. Schmitz, J. Brillo, I. Egry, R. Schmid-Fetzer, Int. J. Mater. Res. 100:11 (2009) 1529-1535.

[S12] W.R. Tyson, W.A. Miller, Surf. Sci. 62 (1977) 267-276.

[S13] L.Z. Mezey, J. Giber, Jap. J. App. Phys. 21:11 (1982) 1569-1571.

[S14] G. Garzel, J. Janczak-Rusch, L. Zabdyr, CALPHAD 36 (2012) 52-56.

[S15] J. Brillo, I. Egry, J. Westphal, Int. J. Mat. Res. 99 (2008) 162-167.

[S16] W. Gasior, Z. Moser, J. Pstrus, J. Phase Equilib. 21 (2000) 167171.

[S17] M. Gündüz, J.D. Hunt, Acta Metall. 33 (1985) 1651-1672.

[S18] K. Dick, T. Dhanasekaran, Z. Zhang, D. Meisel, J. Am. Chem. Soc. 124 (2002) 2312-2317.

[S19] P.R. Couchman, W.A. Jesser, Nature 269 (1977) 481-483.

[S20] Ph. Buffat, J.-P. Borel, Phys. Rev. A 13 (1976) 2287-2298.

[S21] A.N. Goldstein, Appl. Phys. A: Mater. Sci. Process. 62 (1995) 33-37.

[S22] F.G. Meng, H.S. Liu, L.B. Liu, Z.P. Jin, J. Alloys Cmpds. 431 (2007) 292-297.

[S23] R.W. Olesinski, G.J. Abbaschian, Bull. Alloy Phase Diagrams 5 (1984) 180183.

[S24] Y.-B. Kang, C. Aliravci, P.J. Spencer, G. Eriksson, C.D. Fuerst, P. Chartrand, A.D. Pelton, JOM 61 (4) (2009) 7582.

[S25] V.T. Witusiewicz, U. Hecht, S.G. Fries, S. Rex, J. Alloys Cmpds. 385 (2004) 133-143.

[S26] N. Saunders, Al-Cu system, in: I. Ansara, A.T. Dinsdale, M.H. Rand (Eds.), COST-507: Thermochemical Database For light Metal Alloys, European Communities, Luxemburg (1998) 2833.

[S27] A.F. Lopeandía, J. Rodríguez-Viejo, Thermochim. Acta 461 (2007) 82-87.

[S28] V.I. Arkharov, L.M. Magat, Phys. Met. Metallogr. 6(5) (1958) 32-36.

[S29] M. Ellner, K. Kolatschek, B. Predel, J. Less-Common Met. 170 (1991) 171-184.

[S30] C. Kittel, Introduction to Solid State Physics, sixth edition, John Wiley, (1986).

[S31] A. Meetsma, J.L. De Boer, S. Van Smaalen, J. Solid State Chem. 83 (1989) 370-372.

[S32] J. Sun, S.L. Simon, Thermochim. Acta 463 (2007) 32-40.

[S33] D. Mott, J. Galkowski, L. Wang, J. Luo, C-J. Zhong, Langmuir 23 (2007) 5740-5745.

[S34] P. Laty, J.C. Joud, P. Desré, Surf. Sci. 69 (1977) 508-520.

Table S1: Surface area to volume ratio of different shapes of nano-particles.

Geometrical nanostructure	**Size** (a or r)	**Surface Area**	**Volume**	**Ratio of Surface Area/Volume**	**Coefficient of ratio**
Cube	a	$6a^2$	a^3	$\frac{6}{a}$	6
Regular Tetrahedron	a	$\sqrt{3}a^2$	$\frac{a^3}{6\sqrt{2}}$	$\frac{6\sqrt{6}}{a}$	14.7
Hexahedron	a,L; a/L = 1	$(6a^2 + 3\sqrt{3}a^2)$	$\frac{3\sqrt{3}a^3}{2}$	$\frac{4}{\sqrt{3}a}(1+\frac{\sqrt{3}}{2})$	4.3
Regular icosahedron	a	$5\sqrt{3}a^2$	$\frac{5(3+\sqrt{5})a^3}{12}$	$\frac{12\sqrt{3}}{(3+\sqrt{5})a}$	3.97
Sphere	r	$4\pi r^2$	$\frac{4\pi r^3}{3}$	$\frac{3}{r}$	3
Cylinder	r,H; r/H = 1	$4\pi r^2$	πr^3	$\frac{4}{r}$	4

Table S2: Thermodynamic and physical properties used in the calculation of alloy surface tensions and phase diagrams of the Au-Si, Ge-Si, and Al-Cu nanoscale systems (L: Liquid, S: Solid)

Variable	**Function**	**Reference**
Surface tension (J/m^2)	$\sigma_{Au}^{L} = 1.33 - 1.4 \times 10^{-4}\mathrm{T}$	[S4]
	$\sigma_{Au}^{S} = 1.947 - 4.3 \times 10^{-4}\mathrm{T}$	[S5]
	$\sigma_{Si}^{L} = 0.732 - 8.6 \times 10^{-5}(\mathrm{T} - 1687.15)$	[S6]
	$\sigma_{Si}^{S} = 1.510 - 1.589 \times 10^{-4}(\mathrm{T} - 298.2)$	[S7]
	$\sigma_{Ge}^{L} = 0.621 - 2.6 \times 10^{-4}(\mathrm{T} - 1211.4)$	[S8]
	$\sigma_{Ge}^{S} = 1.32 - 2.531 \times 10^{-4}(\mathrm{T} - 298.2)$	[S9]
	$\sigma_{Al}^{L} = 0.871 - 1.55 \times 10^{-4}(\mathrm{T} - 933)$	[S10, S11]
	$\sigma_{Al}^{S} = 1.143 - 1.946 \times 10^{-4}\mathrm{T}$	[S12, S13]
	$\sigma_{Cu}^{L} = 1.615 - 2.3 \times 10^{-4}\mathrm{T}$	[S8]
	$\sigma_{Cu}^{S} = 2.1585 - 4 \times 10^{-4}\mathrm{T}$	[S14]
Molar volume (m^3/mol)	$V_{Au}^{L} = 1.02582 \times 10^{-5} + 7.797 \times 10^{-10}\mathrm{T}$	[S8]
	$V_{Au}^{S} = 1.07109 \times 10^{-5}$	[S8]
	$V_{Si}^{L} = 11.1 \times 10^{-6}[1 + 1.4 \times 10^{-4}(\mathrm{T} - 1687.15)$	[S8]
	$V_{Si}^{S} = 1.206 \times 10^{-5}$	[S9]
	$V_{Ge}^{L} = 13.2 \times 10^{-6}[1 + 8 \times 10^{-5}(\mathrm{T} - 1211.4)$	[S8]
	$V_{Ge}^{S} = 1.365 \times 10^{-5}$	[S9]
	$V_{Al}^{L} = 11.491 \times 10^{-6}[1 + 9 \times 10^{-5}(\mathrm{T} - 933)$	[S15]
	$V_{Al}^{S} = 10.797 \times 10^{-6}[1 + 1.29 \times 10^{-4}(\mathrm{T} - 933)$	[S16]
	$V_{Cu}^{L} = 7.94 \times 10^{-6}[1 + 1 \times 10^{-4}(\mathrm{T} - 1356.15)$	[S8]
	$V_{Cu}^{S} = 7.01 \times 10^{-6} + 2.92 \times 10^{-10}\mathrm{T} + 1.02 \times 10^{-13}\mathrm{T}^2$	[S14]
	$V_{Al_2Cu}^{S} = 9 \times 10^{-6}$	[S17]

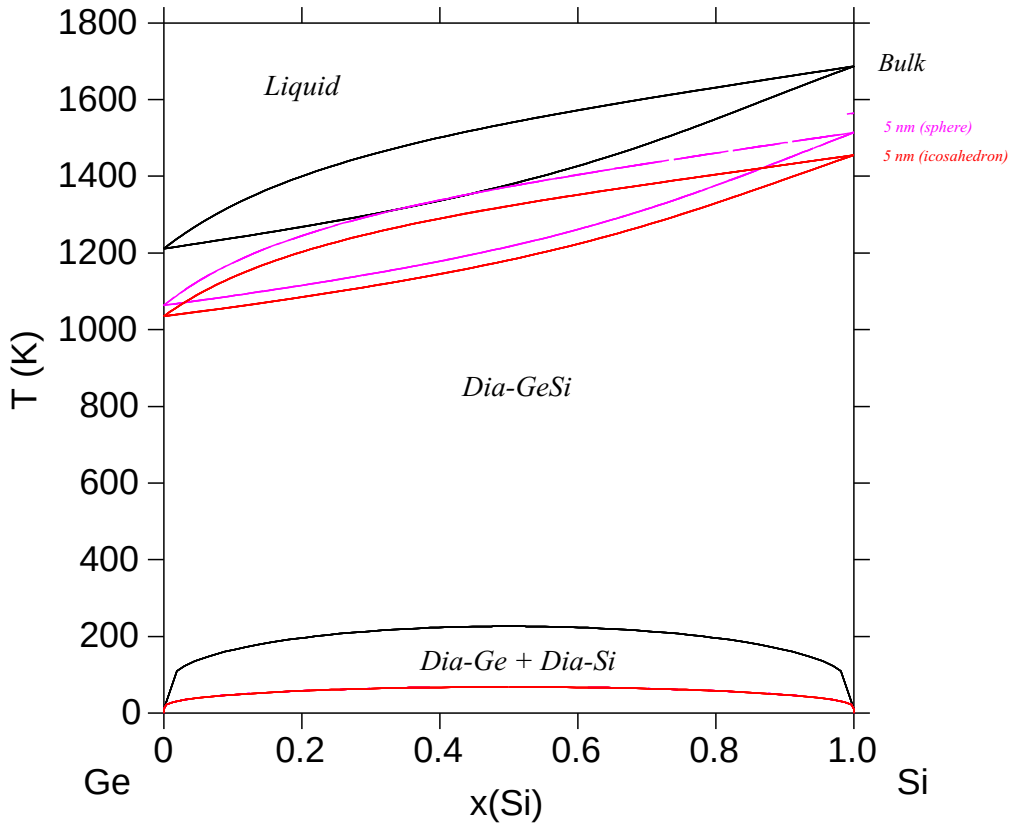

Figure S1: (Color online) Phase diagram of the Ge-Si alloy system calculated for two particle shapes - sphere and a regular icosahedron, both for a particle size of 5 nm, and compared with the bulk phase diagram.

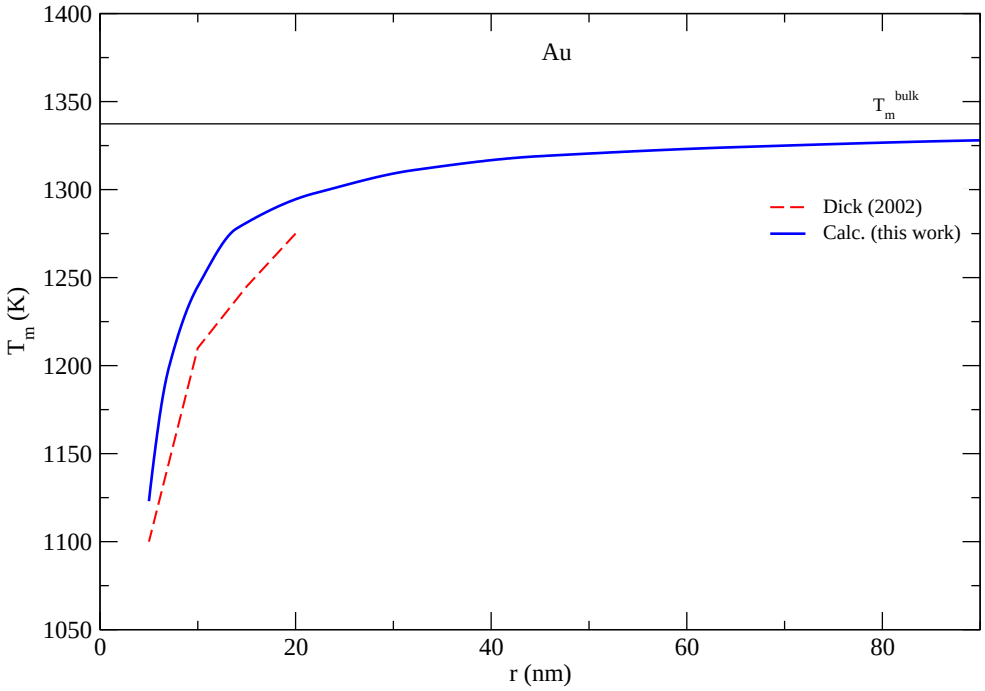

Figure S2: (Color online) Calculated melting points of Au as a function of particle size compared with experimental data from Ref. [S18].

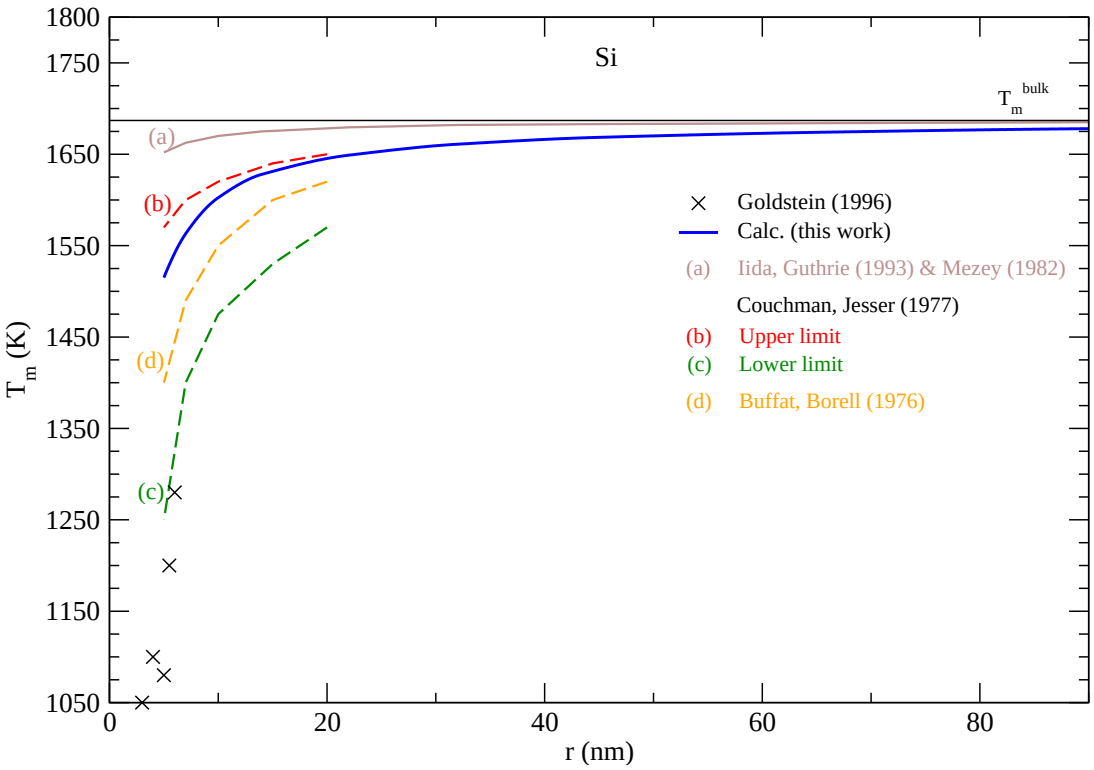

Figure S3: (Color online) Calculated melting points of Si, using surface tension data from Mallot *et al* [S6] for liquid and from Jaccodine *et al* [S7] for the solid phase, as a function of particle size compared with experimental data from Iida & Guthrie [S8], Mezey *et al* [S13], Couchman & Jesser [S19], Buffat & Borell [S20], and Goldstein [S21].

Table S3: Thermodynamic functions used in the calculation of phase diagrams in this work (in J mol^{-1} and K). All bulk and size-independent functions are obtained from (a) Au-Si: SGTE database [S2] and Ref. [S22], (b) Ge-Si: SGTE database [S2] and Refs. [S23] and [S24] for the liquid and diamond phases, respectively, and (c) Al-Cu: Ref. [S25] for the liquid and γD8$_3$ phases, and the COST-507 database [S26] for the rest of the phases.

Standard element reference Gibbs energies

$${}^{o}G_{Au}^{fcc,nano} = {}^{o}G_{Au}^{fcc,bulk} + \frac{6.569\times10^{-5}}{r} - \frac{1.4508\times10^{-8}}{r}.\mathrm{T}$$

$${}^{o}G_{Si}^{dia,nano} = {}^{o}G_{Si}^{dia,bulk} + \frac{5.916\times10^{-5}}{r} - \frac{6.0365\times10^{-9}}{r}.\mathrm{T}$$

$${}^{o}G_{Ge}^{dia,nano} = {}^{o}G_{Ge}^{dia,bulk} + \frac{6.000\times10^{-5}}{r} - \frac{1.0883\times10^{-8}}{r}.\mathrm{T}$$

$${}^{o}G_{Al}^{fcc,nano} = {}^{o}G_{Al}^{fcc,bulk} + \frac{3.419\times10^{-5}}{r} - \frac{8.07\times10^{-10}}{r}.\mathrm{T} - \frac{8.539\times10^{-13}}{r}.\mathrm{T}^2$$

$${}^{o}G_{Cu}^{fcc,nano} = {}^{o}G_{Cu}^{fcc,bulk} + \frac{4.767\times10^{-5}}{r} - \frac{6.847\times10^{-9}}{r}.\mathrm{T} + \frac{3.257\times10^{-13}}{r}.\mathrm{T}^2$$

Liquid phases

$$G_{Au}^{liq,nano} = G_{Au}^{liq,bulk} + \frac{4.093\times10^{-5}}{r} - \frac{1.197\times10^{-9}}{r}.\mathrm{T} - \frac{3.2747\times10^{-13}}{r}.\mathrm{T}^2$$

$$G_{Si}^{liq,nano} = G_{Si}^{liq,bulk} + \frac{2.231\times10^{-5}}{r} + \frac{1.9013\times10^{-9}}{r}.\mathrm{T} - \frac{4.009\times10^{-13}}{r}.\mathrm{T}^2$$

$$G_{Ge}^{liq,nano} = G_{Ge}^{liq,bulk} + \frac{3.347\times10^{-5}}{r} - \frac{6.3326\times10^{-9}}{r}.\mathrm{T} - \frac{8.2368\times10^{-13}}{r}.\mathrm{T}^2$$

$$G_{Al}^{liq,nano} = G_{Al}^{liq,bulk} + \frac{3.207\times10^{-5}}{r} - \frac{1.745\times10^{-9}}{r}.\mathrm{T} - \frac{4.809\times10^{-13}}{r}.\mathrm{T}^2$$

$$G_{Cu}^{liq,nano} = G_{Cu}^{liq,bulk} + \frac{3.325\times10^{-5}}{r} - \frac{8.880\times10^{-10}}{r}.\mathrm{T} - \frac{5.478\times10^{-13}}{r}.\mathrm{T}^2$$

Intermetallic compounds

$$G_{Al:Cu}^{Al_2Cu,nano} = 2 * {}^{o}G_{Al}^{fcc,nano} + {}^{o}G_{Cu}^{fcc,nano} + (-47406 + \frac{3.479\times10^{-5}}{r}) + (6.75).\mathrm{T}$$

Interaction parameters

1. Au-Si

$$L_0^{liq,nano} = (-24103.3028 - \frac{1.5445\times10^{-5}}{r}) + (-15.13883 + \frac{7.4895\times10^{-9}}{r}).\mathrm{T}$$

$$L_1^{liq,nano} = (-29375.2777 + \frac{5.200\times10^{-6}}{r}) + (1.1065 + \frac{1.0399\times10^{-9}}{r}).\mathrm{T}$$

$$L_2^{liq,nano} = (-13032.2412 + \frac{1.5498\times10^{-5}}{r}) - (\frac{4.469\times10^{-9}}{r}).\mathrm{T}$$

2. Ge-Si

$$L_0^{liq,nano} = (+6610 + \frac{2.362\times10^{-6}}{r}) + (-0.354 - \frac{3.596\times10^{-9}}{r}).\mathrm{T}$$

$$L_0^{dia,nano} = (+3765.6 - \frac{1.3823\times10^{-5}}{r}) + (\frac{9.6134\times10^{-9}}{r}).\mathrm{T}$$

3. Al-Cu

$$L_0^{liq,nano} = (-67094 - \frac{9.379\times10^{-6}}{r}) + (8.555 + \frac{4.642\times10^{-9}}{r}).\mathrm{T}$$

$$L_1^{liq,nano} = (32148 - \frac{1.785\times10^{-6}}{r}) + (-7.118 - \frac{5.667\times10^{-10}}{r}).\mathrm{T}$$

$$L_2^{liq,nano} = (5915 + \frac{6.445\times10^{-6}}{r}) + (-5.889 - \frac{1.89\times10^{-9}}{r}).\mathrm{T}$$

$$L_3^{liq,nano} = -8175 + 6.049.\mathrm{T}$$

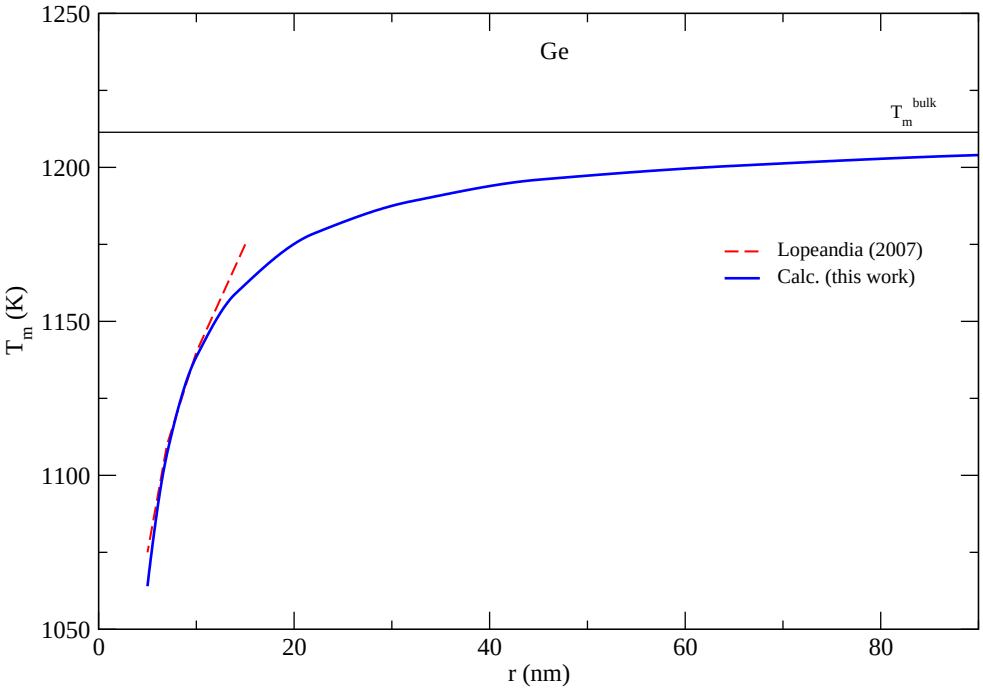

Figure S4: (Color online) Calculated melting points of Ge as a function of particle size compared with experimental data from Ref. [S27].

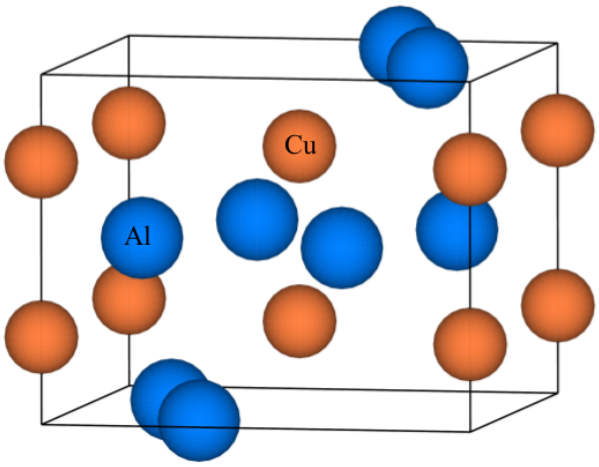

Figure S5: (Color online) Unit cell of the Al_2Cu compound.

Table S4: Calculated lattice constants (in Å) and cohesive energy, E_{coh} (in eV/atom) of Al, Cu, and the Al_2Cu phase from DFT using the LDA approximation. Experimental data are shown in parentheses.

Phase	**Space group**	**Pearson symbol**	**Lattice constants**	**E_{coh} (eV/atom)**
Al	$Fm\bar{3}m$ (no. 225)	cF4	a = 3.9793 (4.047[a])	4.133 (3.39[c])
Cu	$Fm\bar{3}m$ (no. 225)	cF4	a = 3.5246 (3.6536[b])	4.703 (3.49[c])
Al_2Cu	I4/mcm (no. 140)	tI12	a = 5.943 (6.063[d]) c = 4.781 (4.872[d])	-4.506

a: Ref. [S28]

b: Ref. [S29]

c: Ref. [S30]

d: Ref. [S31]

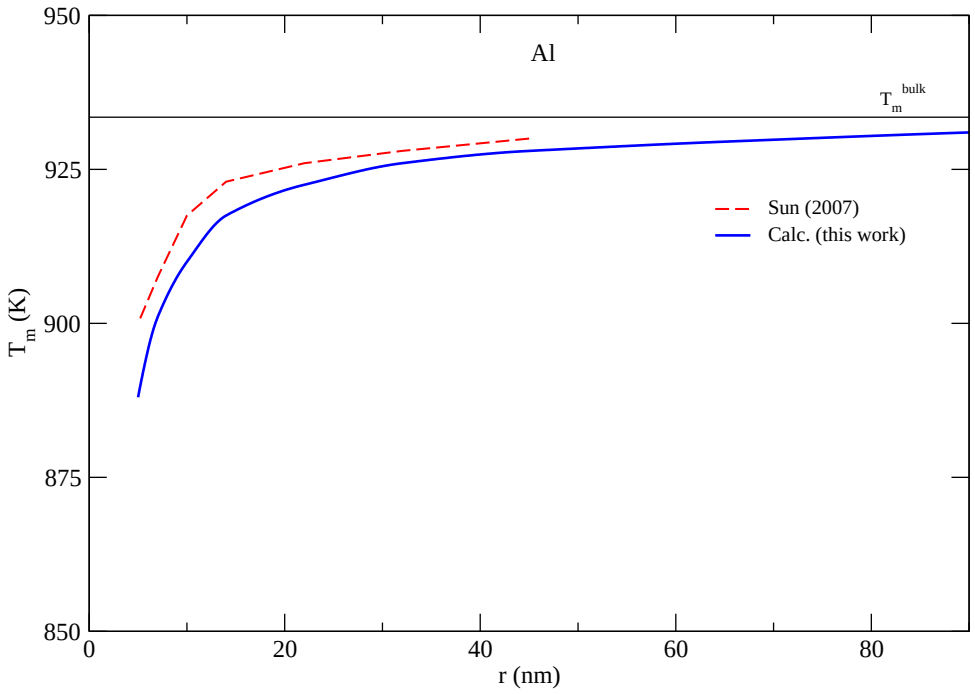

Figure S6: (Color online) Calculated melting points of Al as a function of particle size compared with experimental data from Ref. [S32].

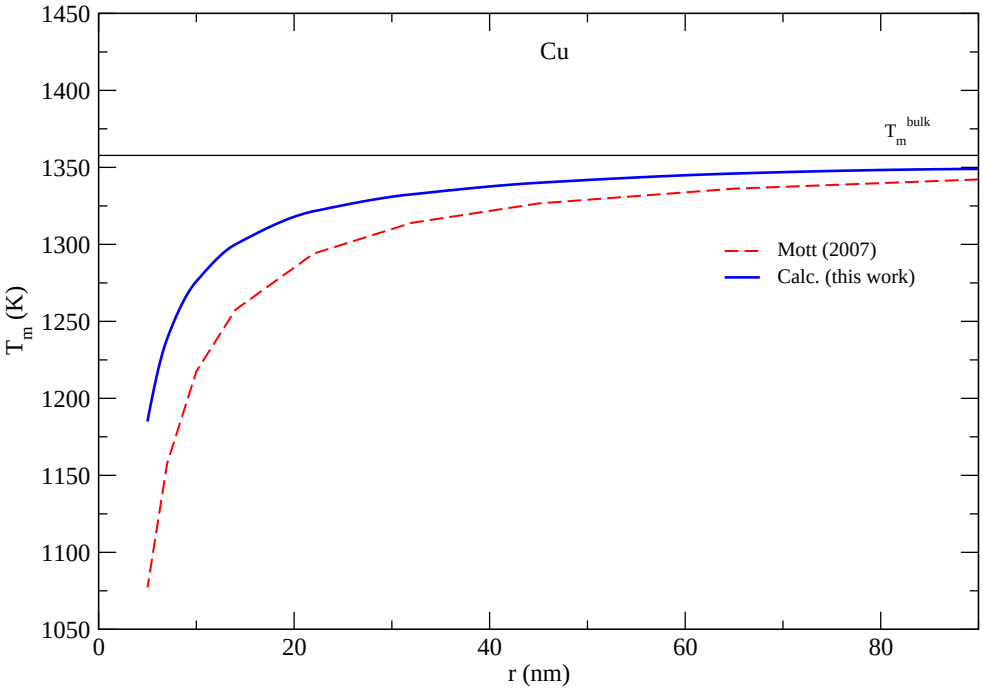

Figure S7: (Color online) Calculated melting points of Cu as a function of particle size compared with experimental data from Ref. [S33].

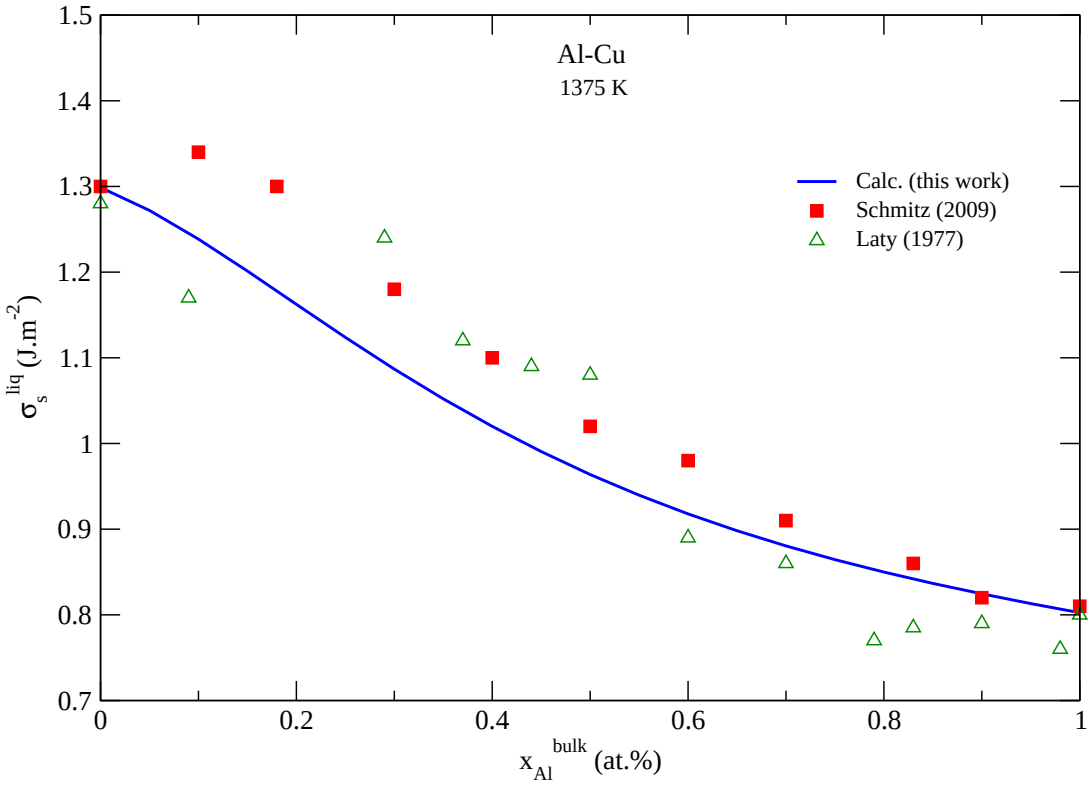

Figure S8: (Color online) Calculated surface tension of the liquid phase in the Al-Cu system compared with experimental data from Refs. [S11, S34].